

Analysis and Calculation of UAV Launch Dynamics from a Catapult System

Phan Đức Đình¹, Bùi Văn Cường¹, and Hoàng Phương Nam¹,
 Lê Đình Lâm¹, Lê Bá Vân, Nguyễn Văn Nam¹.
¹Air Defense – Air Force Academy, Viet Nam
 *Corresponding Author

Abstract: This paper formulates the system of differential equations governing the motion of an unmanned aerial vehicle (UAV) during launch from a catapult system and its subsequent flight until reaching minimum level flight speed. Based on this mathematical model, a computational tool was developed to simulate various launch configurations. The software enables the evaluation of key motion parameters and supports the selection of appropriate input variables for launcher design, ensuring the UAV's safe and effective takeoff.

Keywords: UAV, catapult launch, flight dynamics, motion simulation, launcher design, takeoff safety, differential equations, flight stability.

Date Of Submission: 01-05-2025

Date Of Acceptance: 08-05-2025

I. INTRODUCTION

The launch of an unmanned aerial vehicle (UAV) begins when it starts moving on the launch platform and ends once it reaches the minimum airspeed for stable flight. To reduce launcher size and required thrust P, the departure speed V_{rb} is often set below the minimum flight speed V_{bbmin} , causing the UAV to briefly descend before climbing. A simplified computational model is therefore needed to simulate the launch process and evaluate different scenarios, helping to select optimal design parameters such as launcher length L, thrust P, and launch angle θ .

II. THEORETICAL BASIS

2.1. Initial Parameters

To perform the motion analysis of the UAV during the launch phase, the initial parameters of the system must first be defined. The initial parameters include: thrust generated by the launch system (e.g., pneumatic) P; engine thrust of the UAV T; lift coefficient C_y ; drag coefficient C_x ; moment coefficients m_{z0}, \dots ; wing area S; initial mass of the UAV m_0 ; friction coefficient between the UAV and the launch rail f_{ms} , launch angle θ ; length of the launch rail L; initial altitude of the UAV h_0 ; and fuel consumption rate C_s (per second).

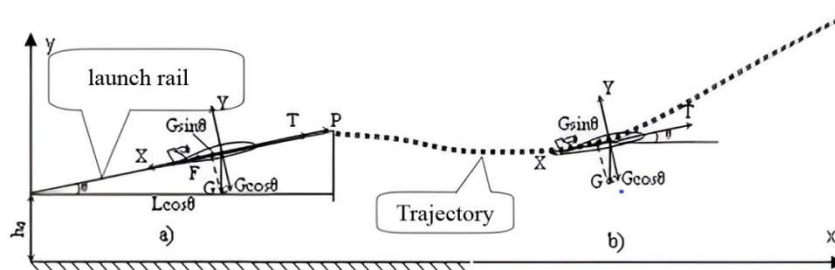


Figure 1.1. Force Diagram and Trajectory of UAV During Launch and Initial Flight Phase

2.2. Forces Acting on the UAV

a) During the UAV's motion along the launch platform (Fig. 2.1):

- Thrust generated by the launch system P;

- Thrust generated by the UAV's engine T;
- Aerodynamic drag Q;
- Friction force along the launch rail F_{ms} ;
- Aerodynamic lift Y;
- Gravitational force $G=mg$;
- Normal force from the launch rail $N= G\cos\theta - Y$.

b) Once the UAV has left the launch platform (Fig. 2.2)

The acting forces include:

- Thrust generated by the propeller engine T;
- Aerodynamic drag Q;
- Aerodynamic lift Y;
- Gravitational force $G=mg$.

2.3. Equations of Motion of the UAV

a) During the UAV's motion along the launch platform (Fig. 2.1):

$$m \frac{dV}{dt} = P + T \cos \alpha - Q - F_{ms} - G \sin \theta$$

$$\frac{d\theta}{dt} = 0$$

$$\frac{dy_0}{dt} = V \sin \theta$$

$$\frac{dx_0}{dt} = V \cos \theta$$

$$\frac{d\omega_{z1}}{dt} = 0$$

$$\frac{d\mathcal{G}}{dt} = 0$$

$$\frac{dm}{dt} = -C_s$$

$$\alpha = \vartheta - \theta$$

where: $Q = \frac{1}{2} C_x \rho V^2 S$; $Y = \frac{1}{2} C_y \rho V^2 S$;

$$F_{ms} = Nf = (G \cos \theta - Y)f .$$

b) Once the UAV has left the launch platform (Fig. 2.2)

$$m \frac{dV}{dt} = T \cos \alpha - Q - G \sin \theta$$

$$mV \frac{d\theta}{dt} = T \sin \alpha + Y - G \cos \theta$$

$$\frac{dy_0}{dt} = V \sin \theta$$

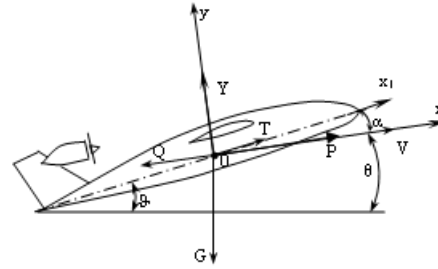


Figure 2.1. Forces Acting on the UAV while the UAV is moving on the launch platform.

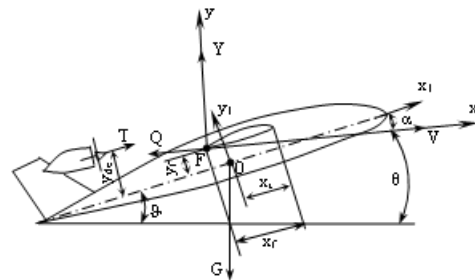


Figure 2.2. Forces Acting on the UAV after leaving the launcher rail

$$\frac{dx_0}{dt} = V \cos \theta$$

$$J_{z1} \frac{d\omega_{z1}}{dt} = m_z \frac{\rho V^2}{2} S b_a$$

$$\frac{d\vartheta}{dt} = \omega_{z1}$$

$$\frac{dm}{dt} = -C_s$$

$$\alpha = \vartheta - \theta$$

where:

m – mass of the UAV, in kilograms (kg);

C_s – fuel consumption rate per second, in kilograms per second (kg/s);

F_{ms} – friction coefficient between the UAV and the launch rail;

S – wing area of the UAV, in square meters (m²);

ρ – air density, in kilograms per cubic meter (kg/m³);

J_{z1} – moment of inertia of the UAV about the z_1 -axis, in kilogram-square meters (kg·m²).

$$m_z = m_{z0} + (C_y \cos \alpha + C_x \sin \alpha)(\bar{x}_l - \bar{x}_f) - (C_x \cos \alpha - C_y \sin \alpha)\bar{y}_f - \bar{C}_T \cdot \bar{y}_{dc} + m_z^\delta \delta + m_z^{\omega_z} \omega_z + m_z^\alpha \dot{\alpha}$$

$$\bar{x}_l = \frac{x_l}{b_a}; \quad \bar{x}_f = \frac{x_f}{b_a}; \quad \bar{y}_f = \frac{y_f}{b_a}; \quad \bar{y}_{dc} = \frac{y_{dc}}{b_a} \text{ – relative lengths as shown in Fig. 2.2;}$$

δ – elevator deflection angle, in radians (rad);

b_a – mean aerodynamic chord of the wing, in meters (m);

C_x – aerodynamic drag coefficient;

C_y – aerodynamic lift coefficient;

C_T – thrust coefficient of the propeller engine;

m_z – pitching moment coefficient about the Oz_1 [2]

m_{z0} – pitching moment coefficient about the Oz_1 -axis at zero lift.

$$m_z^\delta = \frac{\partial m_z}{\partial \delta}$$

$$m_z^{\omega_z} = \frac{\partial m_z}{\partial \omega_z}$$

$$m_z^\alpha = \frac{\partial m_z}{\partial \alpha}$$

III. RESULTS AND DISCUSSION

3.1. Analysis of Launch Angle Effects on UAV Motion

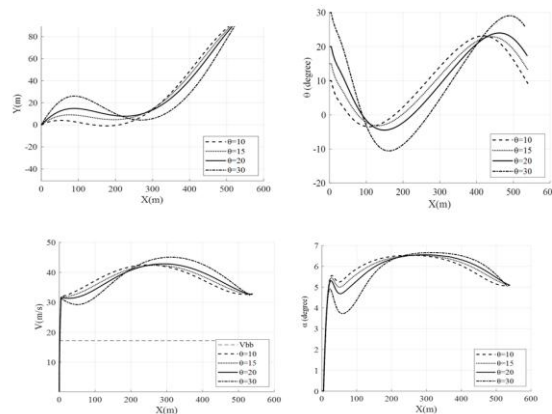


Figure 3.1. Trajectory Analysis of UAV with Respect to Launcher Inclination

The launch angle plays a critical role in determining the initial trajectory and overall flight performance of an unmanned aerial vehicle (UAV). To investigate these effects, simulations were conducted at various launcher inclinations. The corresponding flight trajectories are illustrated in Figure 3.1.

Key observations from the figure are as follows:

- At lower launch angles ($\theta < 15^\circ$), the UAV exits the launcher with relatively high velocity. However, the climb rate is limited, and the risk of premature ground impact increases significantly under such conditions.
- As the launch angle increases ($15^\circ \leq \theta \leq 20^\circ$), the UAV achieves greater altitude shortly after release, while the corresponding reduction in horizontal velocity remains modest. This range is identified as optimal in balancing initial speed and vertical clearance.
- Beyond $\theta = 20^\circ$, further increases in launch angle lead to a marked reduction in altitude gain, likely due to increased drag and suboptimal angle of attack during the initial acceleration phase.
- Across all tested angles, variations in flight path inclination and angle of attack remain within acceptable aerodynamic limits, ensuring flight stability.

It is concluded that the optimal launch angle, considering both safety and performance, lies within the range of 15° to 20° , although specific terrain and mission constraints may necessitate minor adjustments.

3.2. Analysis of the Effects of Launcher Length on UAV Motion

The length of the launch rail significantly influences the UAV's initial acceleration, altitude gain, and overall flight stability. Figure 3.2 presents the UAV trajectories for varying launcher lengths.

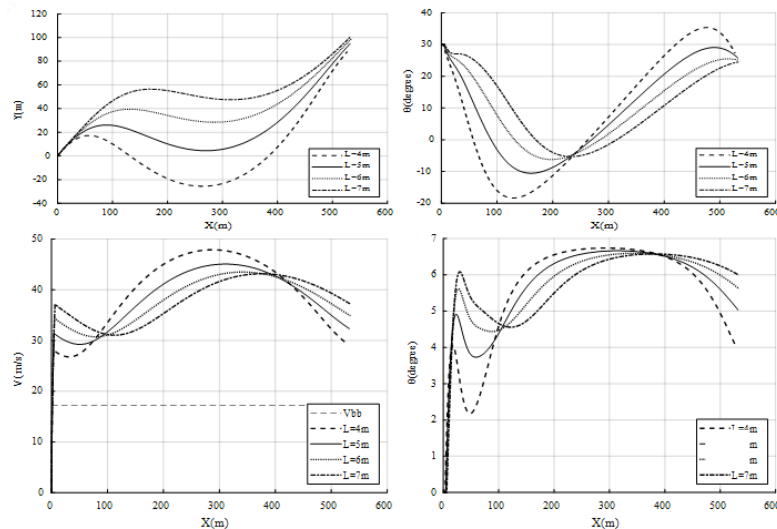


Figure 3.2. Trajectory Analysis Based on Launcher Length

Key observations include:

- When the launch rail is short ($L < 5$ m), the UAV exhibits low exit velocity and suffers considerable altitude loss, increasing the risk of ground contact immediately after launch.
- Increasing the launch rail length enhances initial velocity and reduces post-launch altitude loss, resulting in a more stable and sustained flight trajectory. However, excessively long launch rails introduce practical limitations related to structural complexity, deployment logistics, and spatial constraints.
- Additionally, a shortened launcher leads to a sharp increase in the UAV's angle of attack, which may compromise aerodynamic efficiency during takeoff.
- Based on the trade-off between performance and design feasibility, the optimal launcher length is found to be in the range of 5 to 6 meters.

3.3. Analysis of the Effects of Launcher Thrust on UAV Motion

The effect of increasing launcher thrust is similar to that of extending the launch rail length. A higher thrust improves both the UAV's velocity and altitude after leaving the launcher, while lower thrust results in reduced performance.

- However, unlike launch rail extension, increasing launcher thrust significantly increases the longitudinal overload n_x , which may adversely affect the UAV's structural integrity and its onboard systems. It also introduces challenges in the design and manufacturability of the launch system.

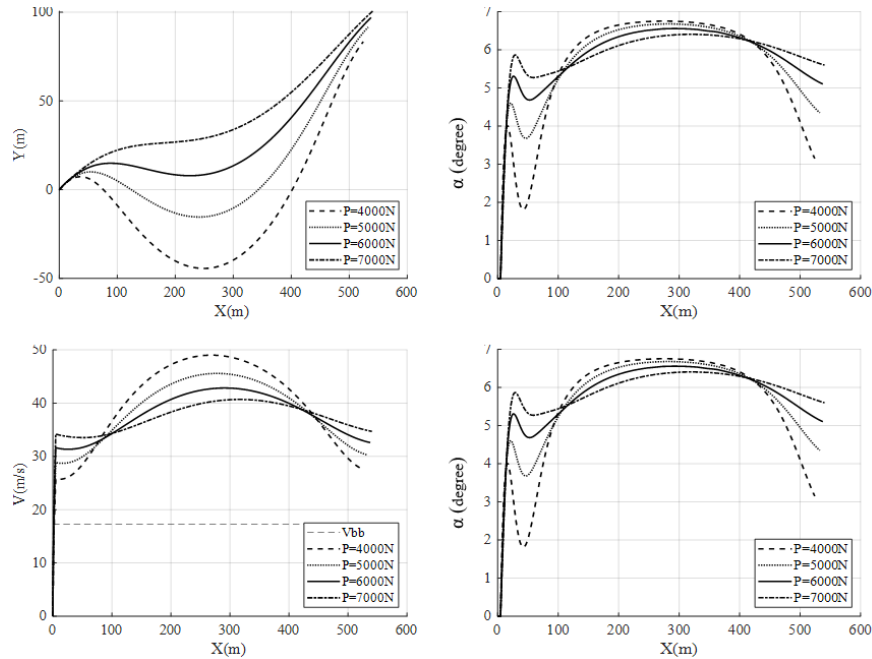


Figure 3.3. Trajectory Analysis of UAV with Varying Launcher Thrust

- The variations in trajectory inclination and angle of attack remain within acceptable bounds, similar to the patterns observed when varying launch rail length.

- Considering performance, safety, and manufacturability, the optimal launcher thrust is recommended to be in the range of 6000–7000 N.

3.4. Analysis of the Effects of Elevator Deflection on UAV Launch Dynamics

Figure 3.4 illustrates the influence of varying elevator deflection angles on the UAV's launch trajectory. This analysis aims to determine how different elevator positions impact the vehicle's pitch behavior, altitude profile, and overall stability during the critical launch phase.

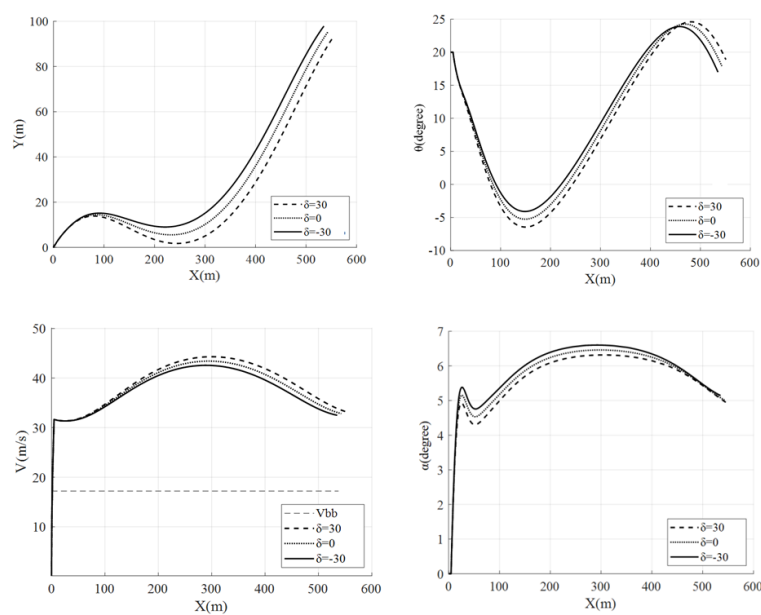


Figure 3.4. Effect of Elevator Deflection Angle on UAV Trajectory

Observations from Figures:

- When the elevator deflection angle is positive (the trailing edge of the elevator deflects downward), increasing the deflection generates a large negative pitching moment, causing the UAV to pitch down and lose altitude significantly, making ground contact more likely.
- Conversely, when the elevator deflection angle is negative (the trailing edge deflects upward), increasing the deflection generates a positive pitching moment, helping maintain altitude while the velocity decreases only slightly.
- The trajectory inclination and angle of attack vary but remain within acceptable limits.
- For effective performance during launch, the elevator deflection angle should be set to $\delta < -15^\circ$ before initiating launch.

3.5. Analysis of UAV Model Launch without Propulsion

During ground testing, a mockup with the same external geometry and mass distribution as the operational UAV can be launched without propulsion. This approach provides a theoretical foundation for evaluating the UAV's motion characteristics during catapult-assisted takeoff, and ensures the overall safety of the launch procedure before deploying the actual UAV.

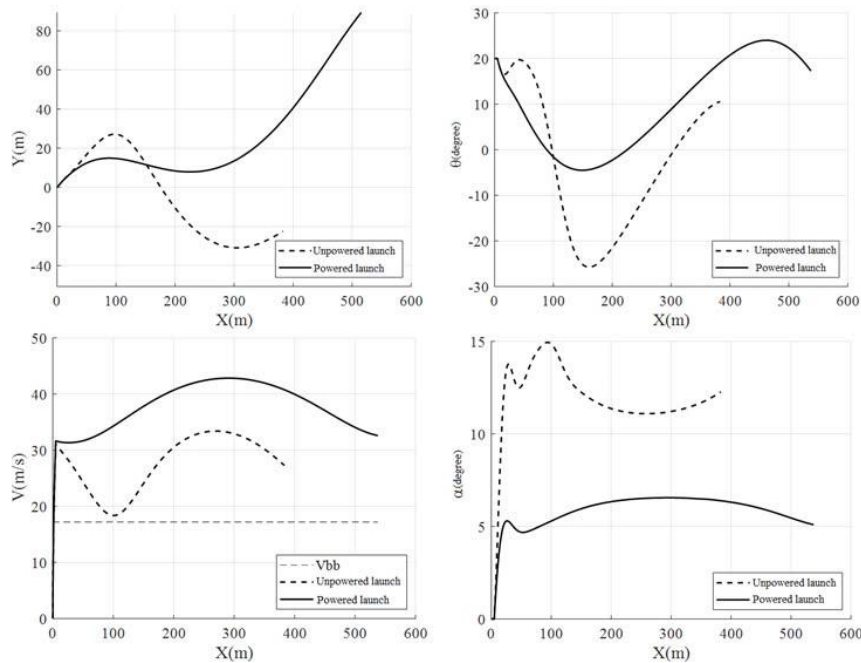


Figure 3.5. Comparison of Powered and Unpowered UAV Launch Trajectories

Key observations from the test results are as follows:

- When launching an unpowered model from ground level (initial altitude $H = 0$), with elevator control surfaces active, the longitudinal stability was found to be satisfactory.
- The flight path inclination exhibited damped oscillations and gradually converged to zero. Simultaneously, the angle of attack remained within acceptable limits, indicating inherent self-stabilizing behavior. The model achieved a glide distance of approximately 180 meters before landing, demonstrating favorable aerodynamic characteristics and confirming the validity of the selected launch configuration.

IV. CONCLUSION

This study examined the influence of launch angle, rail length, launcher thrust, and elevator deflection on UAV takeoff performance. Simulations show that a launch angle between 15° and 20° , a rail length of 5 to 6 meters, and a launcher thrust of 6000–7000 N offer the best balance between altitude gain, velocity, and structural safety. Elevator deflection should be set to $\delta < -15^\circ$ to enhance longitudinal stability. Ground testing with an unpowered mockup confirmed the UAV's stable flight characteristics and validated the launch method. The developed simulation tool supports optimal launcher design and test site selection.

Conflict of interest

There is no conflict to disclose.

FUTURE DEVELOPMENT

Future work will focus on refining the simulation to more accurately model the UAV's pitching motion after launch and incorporating the effects of aerodynamic disturbances. Experimental validation using full-scale models is planned to verify the calculation results. Additionally, the software will be enhanced to support a broader range of launcher configurations and optimize design parameters for different operational environments.

REFERENCES

- [1]. Hoang Luong, "Flight Dynamics and Air Combat Maneuvering of Aircraft", Air Defense – Air Force Academy, 1999.
- [2]. M.V. Cook, "Flight Dynamics Principles", Second Edition, Elsevier, 2007.
- [3]. W.F. Phillips, "Mechanics of Flight", Second Edition, John Wiley & Sons, Inc., 2010.